Two-step hydrothermal synthesis of nano hydroxyapatite particles and their characterization

B. ČOLOVIĆ[a], D. MARKOVIĆ[b], M. PETROVIĆ[b], V. JOKANOVIĆ[a]
[a]*Vinča Institute of Nuclear Sciences, University of Belgrade, Belgrade, Serbia*
[b]*School of Dentistry, University of Belgrade, Belgrade, Serbia*

In this paper, the synthesis and characterization of calcium hydroxyapatite particles, stabilized with poly(ethylene-vinyl acetate) / poly(ethylene-vinyl versatate) (PEVA/PEVV) are presented. The particles were synthesized by two-step hydrothermal method using PEVA/PEVV as a surface-active substance. The structure and crystallinity of the obtained powder were investigated by X-ray diffraction, TEM and HRTEM. The phase identification of hydroxyapatite stabilized with PEVA/PEVV was done by FTIR, while the surface morphology, as well as the size and shape of particles were studied by TEM and AFM. Finally, using MTT and LDH release assays to assess mitochondrial activity and cell membrane integrity, it was confirmed that so synthesized hydroxyapatite powder was not toxic to L929 cells.

(Received January 26, 2014; accepted November 13, 2014)

*Keywords***:** Hydrothermal synthesis, Hydroxyapatite, Ethylene-vinyl acetate/versatate copolymer, TEM, HRTEM

1. Introduction

Calcium hydroxyapatite ($Ca_{10}(PO_4)_6(OH)_2$), CHA) is, among various forms of calcium phosphates, one of the most promising materials for both drug delivery and bone replacement [1]. Due to its excellent biocompatibility, bioactivity and osteoconductivity, this material is suitable for potential orthopedic, dental and maxillofacial applications [1, 2]. However, the application of pure CHA is limited due to its brittleness [3, 4]. Therefore, much attention has been recently focused on the preparation of nanocomposites wherein nano-CHA crystals are dispersed in suitable polymeric matrices. Mechanical properties of these composites can be improved by enhancing the interfacial bonding between the ceramic filler and the polymer matrix. Hence, various methodologies have been developed to improve this bonding [4-9]. Current research efforts are directed towards development of a novel core-shell bioanalogue composite using PEVA/PEVV copolymer as a stabilizing shell agent of previously obtained nanosized CHA particles as core. PEVA/PEVV contains two carboxyl active groups, one with short and the other with long chain length, which can be strongly anchored in CHA surface favoring chemical interactions between the shell polymer and the core CHA surface [10-15].

For the synthesis of such bio-composites, a modified hydrothermal method with application of surface active agents, in this case PEVA/PEVV (applied for the first time in our investigation), proved efficient. This completely new strategy in nano-CHA synthesis has several very important advantages over numerous known methods of CHA synthesis, such as chemical methods of precipitation, sol-gel or calcium phosphates hydrolysis. The obtained structures have a great ability to attach to antibodies and biomarkers, such as pentosidine, which can be targeted as a drug delivery system to osteoporotic bone [16]. Investigations can also be directed towards covering the CHA core with magnetic nanoparticles, and their subsequent modification with PEVA/PEVV shell. This can be a suitable solution for the guidance of these delivery systems to the targeted area by an external magnetic field (EMF). The advantages of such CHA- PEVA/PEVV structures, from the aspect of bone tissue engineering, are stronger inter-bonding of these structures and their bonding inside of scaffold built out of these nanosized constitutive elements. Both of them result in better mechanical scaffold properties and its biological activity. On the other hand, potential multifunctional properties of these systems are very useful for their application as targeted drug delivery systems [17].

The main aim of this study was to prepare CHA particles stabilized with coupling agent by combining two methods: the first one was hydrothermal synthesis as the most promising way to obtain crystallized CHA at nano level and the second one was the preparation of very small CHA particles, using surface active substance PEVA/EVV. PEVA-PEVV was chosen because its toxicity is negligible and its application for biomedical purposes is well-known (drug delivery systems) [10-15].

2. Experimental procedure

2.1. Synthesis of CHA

Powders of calcium oxide CaO from eggshell and $(NH_4)_2HPO_4$ (p.a, Merck), were used for the hydrothermal synthesis of HA. The chicken eggshells were first calcined at 900 °C, until complete removal of carbon, *i.e.*, dissociation of $CaCO_3$ to CaO. Using adsorption atomic spectroscopy (PerkinElmer 3030B), the concentrations of

Ca, Mg and P contained in the egg shells were found to be: 38.38 mass%, 1.11 mass% P 0.2 mass%, respectively. The loss of the inorganic part of the egg shells, as CO_2, was 60.3 mass%.

The precursor solutions were prepared as a combination of two mixtures: i) 500 ml of a 3.02 cmol aqueous solution of $Ca(OH)_2$ (mixture 1) and 500 ml of a 2.32 cmol aqueous solution of $(NH_4)_2HPO_4$ (mixture 2). The $(NH_4)_2HPO_4$ mixture was poured into vigorously stirred $Ca(OH)_2$ mixture. Finally, 0.1 M HCl or $(NH_4)OH$ solution was added into the so-prepared solution to adjust its pH to 7.4. This solution was put in a beaker, covered with a watch glass and autoclaved at a temperature of 150 °C under a pressure of $5 \cdot 10^5$ Pa for 8 h. After the hydrothermal treatment in the autoclave, the precipitate was decanted, dried at 80 °C for 48 h, ground, washed with deionized water, and ultracentrifuged in order to obtain the purest possible CHA.

The next step was to make a mixture of 5 g of hydrothermally synthesized CHA and 1.5 g of PEVA/PEVV for further processing in the autoclave at a temperature of 120 °C for 2 h. The obtained particles were filtrated through a filter with a pore size of 200 nm.

2.2. Characterization of CHA

The X-ray diffraction (XRD) technique (Philips PW 1050 with Cu-$K_{\alpha 1-2}$ radiation) was used for phase analysis of CHA and determination of its crystallite sizes and lattice parameters. The data were obtained in the 2θ range from 9 to 67° with a scanning step of 0.05° and exposition time of 2 sec per step. The size of hydroxyapatite nanocrystallites was obtained by using the Sherrer equation $d = K\lambda/B\cos\theta$, where d (in nm) is the average diameter of crystallites, K the shape factor, B the width of the (002) diffraction peak at half maximum height, λ the wavelength of the employed X-rays, and θ is the Bragg diffraction angle. The lattice parameters were extracted from the experimental XRD data using FULLPROF program (in a full-profile matching mode).

The CHA powder was also characterized by employing a Perkin Elmer 983G IR spectrometer using the KBr pellet technique in the wave number range from 4000 to 400 cm^{-1}.

The samples for TEM and HRTEM study were deposited on a copper-grid-supported perforated transparent carbon foil. They were analyzed using a field-emission electron-source transmission electron microscope (JEOL 2010 F), equipped with an energy-dispersive X-ray spectrometer (LINK ISIS EDS 300) operated at 200 kV and a multiscan CCD camera (Gatan Model 794) for digital image recording with 1024 x 1024 pixel resolution. The goniometer tilt and the CCD camera were controlled automatically.

The microscope is also equipped with an ultrahigh resolution configuration: point-to-point resolution of 0.194 nm and lattice resolution of 0.14 nm. A microbeam diameter of 0.5 nm can be obtained that allows for nanobeam electron diffraction and CBED, as well as high-spatial resolution X-ray analysis.

The specific issues related to crystal orientation in HRTEM were particularly considered. Namely, the usually present Kikuchi lines in crystallographic specimens, (which serve as "roads in orientation-space" for microscopists because they connect zone axes that share family of planes), can not be easily seen under parallel nor under convergent beam illumination (due to the high density of excited reflections visible on the apatite pattern in normal selected area). Therefore, the observed crystal position is adjusted by the double-tilt holder to create Laue circles which intersect the central spot. The tangent line that touches the circles and passes through the central spot precisely determines the tilting axis of the holder (usually referred to as the α tilt), as well as the second tilt axis, or β tilt, perpendicular to this line. The results indicate that the tilt direction for the α/β holder lies at 22 ± 0.5° from the horizontal axis. This holder position is optimally adjusted for observation of characteristic diffraction plane of hydroxyapatite. Similar approach with full theoretical explanation can be found in literature [18].

2.3. Cell viability assessment

For the cell viability analysis, L929 mouse fibroblasts (European Collection of Animal Cell Cultures, Salisbury, UK) were incubated in control and CHA-coated 6-well cell culture plates (1 x 10^6 cells/well) for 48 h at 37 °C in a humidified atmosphere with 5 % CO_2, in a HEPES-buffered RPMI 1640 cell culture medium supplemented with 5 % fetal bovine serum, 1 mM sodium pyruvate and 10 ml/L penicillin/streptomycin (all from Sigma-Aldrich, St. Louis, MO). The measurement of mitochondria-dependent reduction of 3-(4,5-dimethylthiazol-2-yl)-2,5-diphenyltetrazolium bromide (MTT) to formazan as an indicator of the mitochondrial dehydrogenase activity, and the release of the intracellular enzyme lactate dehydrogenase (LDH) as a marker of cell membrane damage, were used to determine cell viability exactly as previously described. The cell morphology was assessed using an inverted phase contrast microscope (Leica Microsystems, Wetzlar, Germany). The statistical significance of the differences in cell viability between control and SiO_2-exposed cells was analyzed by two-tailed Student's t-test and a p value of less than 0.05 was considered significant.

3. Results and discussion

3.1. XRD analysis

The X-ray diffraction pattern of hydrothermally synthesized powder is shown in Fig.1. As can be seen, the synthesized powder corresponds to carbonated calcium hydroxyapatite (CO_3HA) [19], because all characteristic diffraction patterns are present, *i.e.*, (002) at 2θ=25.86, (121) and (211) at 2θ=31.9; (112) at 2θ=32.26, (300) at

2θ=33.12, (222) at 2θ=46.86, and (213) at 2θ=49.58. The average crystallite size obtained by using the Sherrer formula was 16 nm. The lattice parameters of the hexagonal CHA (space group $P6_3/m$) were extracted from the experimental XRD data using FULLPROF program (in a full-profile matching mode), and it was found a = b = 9.41(1) Å and c = 6.85(1) Å.

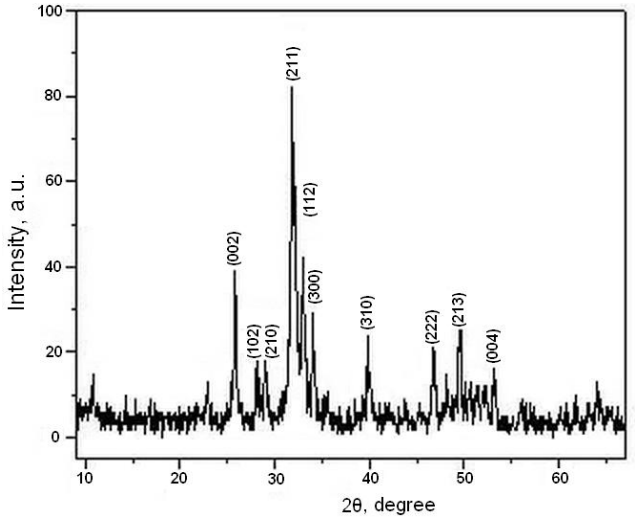

Fig.1. X-ray patterns of hydrothermally synthesized CHA

3.2. IR analysis

IR spectrum of CHA powder stabilized with PEVA/PEVV is given in Fig.2. A broad band between 3436 cm^{-1} (small shoulder) and 3154 cm^{-1} can be attributed to the OH stretching vibration, which belongs to various hydroxyl groups present in CHA-PEVA/PEVV. The band at 2873 cm^{-1} corresponds to the ν(C-H) symmetric stretching vibrations of intercalated PEVA/PEVV at the surface of the CHA particles. A strong peak at 1731 cm^{-1} can be assigned to the stretching mode vibration of ester of the carboxyl group C=O, which is shifted from its ideal position for pure PEVA/PEVA to 1750 cm^{-1} and is of lower intensity. The band at 1639 cm^{-1} is ascribed to the bending mode of OH vibrations of interlayered water. A broad and low-intense band at 1555 cm^{-1} can be attributed to very weak, asymmetric νCO vibration of verstaile and/or acetate group [10-15, 19].

A narrow and intense band at 1406 cm^{-1}can be assigned to the CO_3^{2-} group of B-type CO_3HA, with corresponding formula $Ca_{9.7}Mg_{0.3}(PO_4)_{6-x}(CO_3)_x(OH)_2$ (AAS analysis showed presence of Mg in starting chemicals). It can also be attributed to the dimeric δOH vibration of versatate acid. A broad and intense band at 1075 cm^{-1} can be assigned to the ν_3 asymmetric stretching vibration of PO_4^{3-}. Inside of the band for phosphate group of CHA, the band at 1026 cm^{-1} corresponding to the C-O stretching mode of ethylene-vinyl acetate is probably hidden. The shoulder at 976 cm^{-1} is assigned to the ν_1 symmetric stretching mode of PO_4^{3-} vibration, while the vibration at 885 cm^{-1} belongs to the stretching mode of CO_3^{2-} ions in CHA. This band can also be an indication of the presence of HPO_4^{2-} group. A slightly pronounced band at 723 cm^{-1}, can probably be ascribed to ethylene backbone of PEVA/PEVV chains and their angular deformations. The band at 611 cm^{-1} corresponds to the liberation mode of the OH vibration strongly shifted towards smaller wave numbers. Bands at 561 cm^{-1} and 477 cm^{-1} are attributed to the ν_2 symmetric stretching mode of PO_4^{3-} vibration [10-15, 19].

All these more or less shifted bands ascribed to various characteristic vibrations of CHA and PEVA/PEVV, including particularly vibrations of hydroxyapatite OH groups, are obviously a significant evidence for strong chemical interactions between CHA and PEVA/PEVV at their interface. They clearly show strong interface bonding between CHA and PEVA/PEVV in specific stable structure, which might be promising for various medical applications, as discussed in introduction of this paper.

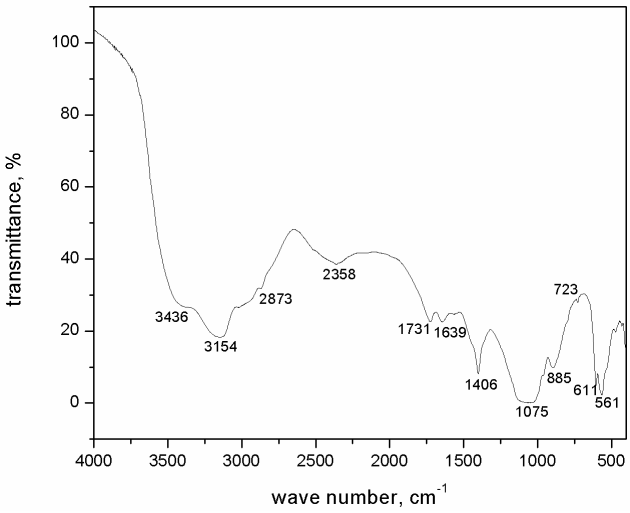

Fig.2. IR spectra of hydrothermally synthesized CHA stabilized with PEVA/PEVV

3.3. TEM investigations

TEM study revealed crystalline particles, interconnected in the form of agglomerates, with sizes mostly of about several microns. They have platelet like shape, with areas of different number densities of particles (Fig.3). This anisotropic shape of particles is probably caused by specific interconnection of basic particles under given conditions of hydrothermal treatment. The sizes of basic particles are between 20 and 40 nm, showing satisfying agreement with XRD measurements (the differences between particle and crystallite sizes measured by XRD show that particles consist of more than one crystallite).

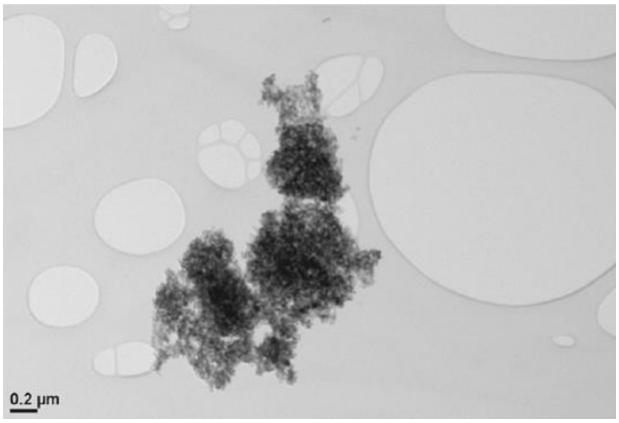

Fig.3. TEM image of CHA particles.

HRTEM image shows no amorphous layer at the surfaces of the crystalline nanoparticles (Fig.4). The inset in Fig.4 shows one representative ring electron diffraction pattern, obtained from the region presented in the same figure. This ring pattern was indexed to the hexagonal hydroxyapatite structure and Miler indices were marked.

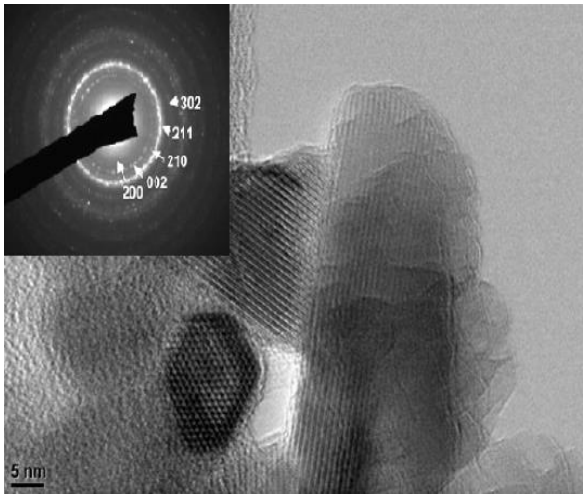

Fig.4. HRTEM image of CHA particles.

Besides, EDS analysis (Fig.5) showed only Ca, P and O (Ca/P=1.61). This value confirms that CHA is slightly calcium deficient. This result fairly matches with results of IR spectrum, in which band at 885 cm^{-1} indicates the presence of HPO_4^{2-}, characteristic for calcium deficient apatite.

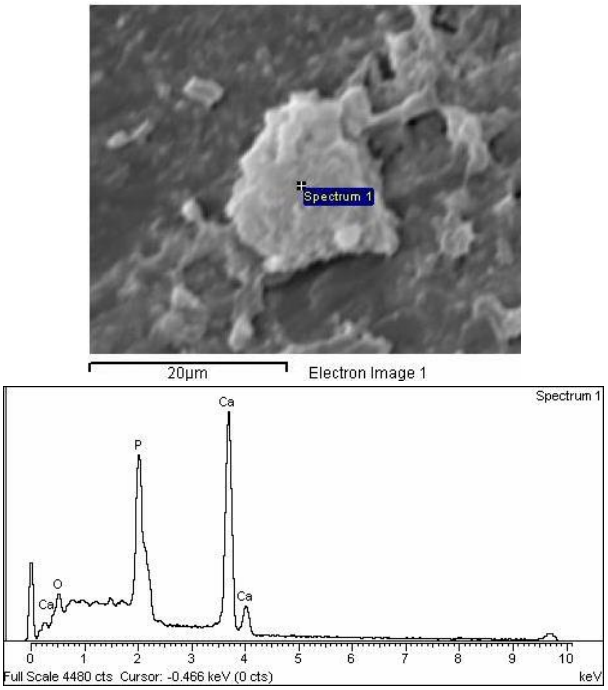

Fig.5. EDS analysis of synthesized CHA

3.4. The effect of CHA on cell viability

The effect of CHA powder, stabilized with PEVA/PEVV surface active substance, on cell viability was analyzed using inverted phase contrast microscopy and LDH and MTT viability assays.

The incubation of L292 fibroblasts in CHA-coated cell culture plates for 48 h did not cause any significant change in cell morphology, as confirmed by inverted phase contrast microscopy (Fig.6A).

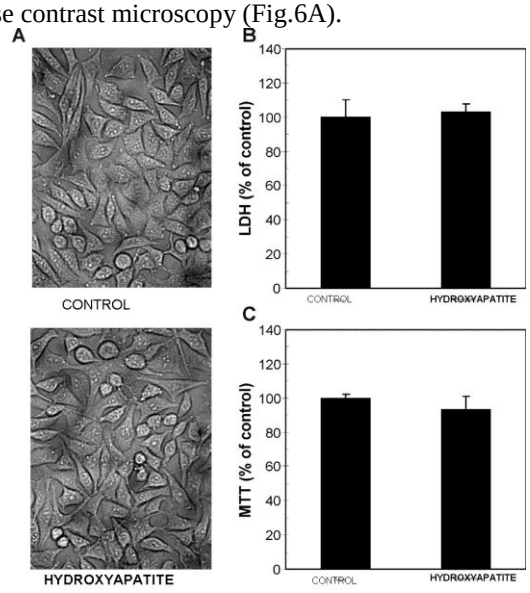

Fig.6. The effect of CHA on cell viability. (A-C) L929 cells were incubated for 48 h in control (uncoated) and CHA-coated plates. Cell morphology was examined by phase contrast microscopy (A), while cell viability was determined by LDH release assay (B) or MTT test (C). The results in (B) and (C) are mean ± SD values of triplicates from a representative of three experiments ($p > 0.05$, t-test).

Accordingly, the concentration of LDH in the supernatant of L292 cell cultures did not increase in CHA-coated compared to control plates (Fig.6B), thus confirming the absence of cell membrane damage. Also, the MTT assay revealed no significant differences in mitochondrial dehydrogenase activity measured in L929 cells in CHA-coated compared to control plates (Fig.6C).

4. Conclusion

The synthesis and characterization of CHA particles stabilized with PEVA/PEVV were presented in this work. The synthesis of these particles was done as a modification of typical hydrothermal synthesis of CHA by addition of PEVA/PEVV as a surface-active substance. To the best of our knowledge, PEVA/PEVV was used for the first time in literature to modify the CHA surface. Based on XRD measurements, the formation of very small crystallites with a diameter of 16 nm was established. The CHA particle sizes obtained by TEM were 20-40 nm and agglomerate sizes were from 100 nm to several microns. The results obtained by IR spectroscopy showed the presence of all bands characteristic for CHA and PEVA/PEVV, as well as a very strong chemical interaction at the interface between of CHA and PEVA/PEVV.

By using phase contrast microscopy to analyze cell morphology, as well as MTT and LDH release assays to assess mitochondrial activity and cell membrane integrity, it was confirmed that CHA synthesized on the presented way was not toxic to L929 cells.

Acknowledgement

This work was supported by the Ministry of Science and Technology of the Republic of Serbia through project No. 172026.

References

[1] A.K. Jain, R. Panchagnula, International Journal of Pharmaceutics, **206,** 1 (2000).
[2] J. Chevalier, L. Gremillard, Journal of the European Ceramic Society, **29,** 1245 (2009).
[3] S.C. D'Andrea, A.Y. Fadeyeev, Langmuir, **19,** 7904 (2003).
[4] R.A. Sousa, R.L. Reis, A.M. Cunha, M.J. Bevis, Composites Science and Technology**, 63,** 389 (2003).
[5] C.M. Vaz, R.L. Reis, A.M. Cunha, Biomaterials, **23,** 629 (2002).
[6] J. Klinkaewnarong, E. Swatsitang**,** S. Maensiri**,** Solid State Sciences, **11,** 1023.
[7] R.E. Riman, W.L. Suchanek, K. Byrappa, C.W. Chen, P. Shuk, C.S. Oakes, Solid State Ionics, **151,** 393 (2002).
[8] M. Chen, J. Tan, Y. Lian, D. Liu, Applied Surface Science, **254,** 2730 (2008).
[9] O.C. Wilson Jr., J.R. Hullb, Materials Science and Engineering, *C* **28,** 434 (2008).
[10] N. Pramanik, S. Mohapatra, P. Bhargava**,** P. Pramanik**,** Materials Science and Engineering C, **29,** 228 (2009).
[11] V. Goodarzi, S.H. Jafari, H.A. Khonakdar, S.A. Monemian, M. Mortazavi, Polymer Degradation and Stability, **95,** 859 (2010).
[12] Y. Lin, J. Wang, D.G. Evans, D. Li, J. Phys. Chem. Solids, **67,** 998 (2006).
[13] G. Socrates, Infrared characteristic group frequencies tables and charts, John Wiley & Sons, Chichester, 1994.
[14] P. Opaprakasit, M. Opaprakasit, P. Tangboriboonrat, Appl. Spectrosc., **61,** 1352, (2007).
[15] E.G. Palacios, A.J. Monhemius, Hydrometallurgy, **62,** 135, 2001.
[16] M. Saito, S. Mori, T. Mashiba, S. Komatsubara, K. Marumo, Osteoporosis International, **19,** 1343 (2008).
[17] S.I. Doronin, E.B. Feldman**,** S. Lacelle**,** Chemical Physics Letters, **353,** 226 (2002).
[18] M. Espanol, J. Portillo, J. Manero, M. Ginebra, Cryst. Eng. Comm., **12,** 3318 (2010).
[19] V. Jokanović, B. Jokanović, D. Marković, V. Živojinović, S. Pašalić, D. Izvonar, M. Plavšić, Mat. Chem. Phys., **111,** 180 (2008).

Corresponding author: vukoman@vin.bg.ac.rs